Magnetic Resonance Imaging of the Temporomandibular Joint Disc: Feasibility of Novel Quantitative Magnetic Resonance Evaluation Using Histologic and Biomechanical Reference Standards

Hatice T. Sanal, MD
Associate Professor
Department of Radiology
Gulhane Military Medical Faculty
Ankara, Turkey

Won C. Bae, PhD
Assistant Professor
Department of Radiology
University of California–San Diego
San Diego, California, USA

Chantal Pauli, MD
Research Associate
Shiley Center for Orthopedic Research and Education at Scripps Clinic
La Jolla, California, USA

Jiang Du, PhD
Associate Professor

Sheronda Statum, MS
Senior Research Associate

Richard Znamirowski, BS
Magnetic Resonance Technologist
Department of Radiology

University of California–San Diego
San Diego, California, USA

Robert L. Sah, MD, ScD
Professor
Department of Bioengineering
University of California–San Diego
La Jolla, California, USA

Christine B. Chung, MD
Professor
Department of Radiology
University of California–San Diego, and
VA San Diego Healthcare System
San Diego, California, USA

Correspondence to:
Christine B. Chung
Department of Radiology
University of California–San Diego
200 W Arbor Drive
San Diego, CA 92103, USA
Fax: (858) 822-1614
Email: cbchung@ucsd.edu

Aims: *To use the ultrashort time-to-echo magnetic resonance imaging (UTE MRI) technique to quantify short T2* properties (obtained through gradient echo) of a disc from the human temporomandibular joint (TMJ) and to corroborate regional T2* values with biomechanical properties and histologic appearance of the discal tissues.* ***Methods:*** *A cadaveric human TMJ was sliced sagittally and imaged by conventional and UTE MRI techniques. The slices were then subjected to either biomechanical indentation testing or histologic evaluation, and linear regression was used for comparison to T2* maps obtained from UTE MRI data. Feasibility of in vivo UTE MRI was assessed in two human volunteers.* ***Results:*** *The UTE MRI technique of the specimens provided images of the TMJ disc with greater signal-to-noise ratio (~3 fold) and contrast against surrounding tissues than conventional techniques. Higher T2* values correlated with lower indentation stiffness (softer) and less collagen organization as indicated by polarized light microscopy. T2* values were also obtained from the volunteers.* ***Conclusion:*** *UTE MRI facilitates quantitative characterization of TMJ discs, which may reflect structural and functional properties related to TMJ dysfunction.* J OROFAC PAIN 2011;25:345–353

Key words: indentation, magnetic resonance imaging, osteoarthritis, temporomandibular joint disc, ultrashort time-to-echo

Although it shares common features with other synovial joints through similar structure, including the presence of an intra-articular disc, a deep synovial and superficial fibrous capsule, and stabilizing ligamentous structures, the temporomandibular joint (TMJ) is unique in many ways. One striking feature is the presence of fibrocartilage rather than hyaline cartilage covering its articulating surfaces.[1] Owing to the important functions in which it participates (eg, mastication and speech), an understanding of the complex anatomy of this articulation and knowledge of its common pathology are crucial.[2] With regard to the latter, current medical perspectives related to temporomandibular disorders involve orthopedic principles combined with a biopsychosocial understanding of how chronic pain disorders affect those who have them.[3,4] Currently, magnetic resonance imaging (MRI) is accepted as the most accurate means of noninvasive evaluation of the soft tissues of the joint.[5–9] This has been recently reinforced by Ahmad et al,[4] who concluded that standard clinical MRI reliability was excellent for diagnosis of disc displacements and synovial effusion, but performed poorly for the detection of osteoarthritis.

Several MRI techniques have been introduced to improve visualization of TMJ anatomy.[5,7,8,10–14] However, significant challenges remain because of the fibrocartilaginous nature of TMJ soft tissues comprised

largely of short T2 components, an intrinsic magnetic resonance (MR) property that makes their MRI evaluation technically challenging. MRI evaluation of the osseous structures of the TMJ, such as subchondral and cortical bone, are further complicated by even shorter intrinsic T2 values and structural considerations requiring very high in-plane resolution for visualization. With the ultrashort time-to-echo (UTE) MR pulse sequence, it is possible to detect short T2 relaxation components in tissues before they decay to a level where they are not detected with conventional spin-echo pulse sequences.[15–21]

The aims of this study were to use the UTE MRI technique to quantify short T2* properties (obtained through gradient echo rather than spin echo) of a disc from the human TMJ and to corroborate regional T2* values with biomechanical properties and histologic appearance. Preliminary results of the 3T UTE MRI technique and its feasibility to acquire signal from the short T2 tissue of the TMJ disc are presented, thereby affording the opportunity to visually characterize and to provide previously unknown quantitative T2* measurements. The quantitative data of the intrinsic T2* properties of any tissue can be used to calculate optimal time-to-repeat (TR), time-to-echo (TE), and flip angle for MR sequences that will allow optimization for signal and contrast. In addition, preliminary data are presented which suggest that UTE quantitative MR evaluation of tissue may provide a noninvasive means to detect intrinsic structural alteration and alteration of tissue material property by using histologic and biomechanical reference standards.

Materials and Methods

This cadaveric and in vivo study was approved by the authors' institutional review board, and informed consent was obtained from the human volunteers.

Tissue Preparation

A unilateral TMJ was removed en block from the skull of a fresh male cadaver, aged 79 years at death. The specimen was harvested in a closed-mouth intercuspal position of the subject's natural teeth. There was no information available concerning the existence of TMJ disease before death.

The tissue block was extracted by a band saw with a fine-toothed metal blade (Exact, Apparatebau). Reference landmarks included the nasal septum, the orbital ridge, the nasolabial fold, and the retroauricular eminence. The resultant tissue block was sectioned in a true sagittal plane through the TMJ. The reference angle was extrapolated from MR images and based on the orientation of the TMJ with respect to the nasal septum. Sections were acquired at 3-mm slice thickness and were photographed digitally. They were subsequently frozen to –40°C in an ultralow freezer (Bio-Freezer; Forma Scientific). The specimens were allowed to thaw for 3 hours at room temperature prior to MRI.

Ex Vivo MRI Evaluation

MRI was performed on a 3T MRI system (Signa; GE Medical Systems) with a 3-inch surface coil placed in contact with the specimen slices. Two central sagittal slices from the TMJ were imaged (Fig 1). UTE MRI was used to perform novel MR pulse sequences. These included a standard dual-echo UTE sequence as well as a multiecho UTE sequence using a constant TR-variable TE technique for T2* quantification. Standard clinical MR sequences were acquired, including T1-weighted and proton density fat-suppressed spin-echo images.

Parameters for T1-weighted spin-echo sequences included TR = 500 ms, TE = 15 ms, matrix = 512 × 512, slice thickness = 2 mm, number of excitations (NEX) = 4, and a field of view (FOV) = 8 cm. Proton density-weighted fat-suppressed images were acquired using the following parameters: TR = 1,800 ms, TE = 11.7 ms, matrix = 512 × 512, slice thickness = 2 mm, NEX = 4, and FOV = 8 cm.

For UTE MRI, the basic pulse sequence employs a half radiofrequency excitation followed by radial imaging of k-space from the center out.[10–12] This was followed by another half radiofrequency excitation with the gradient reversed and repeated radial mapping. The two sets of data were added to give a single line of k-space and the process was repeated through 360 degrees in 512 steps. The data were mapped onto a 512 × 512 grid and reconstructed by two-dimensional Fourier transformation (2DFT) to give a gradient echo-like image. Two sets of images with TEs of 8 μs, 6.6 ms were produced with a TR of 500 ms. Frequency-based fat suppression was employed.

Standard clinical and UTE MR sequences were assessed visually and through measurement of signal-to-noise (SNR) values. The region of interest (ROI) was placed in the TMJ disc tissue as well as in regions of noise outside the tissue slice. ROIs were cut and pasted at the MR scanner to ensure identical size and placement from sequence to sequence.

To characterize T2* values in the TMJ disc, a Constant TR–Varying TE technique was used in conjunction with UTE MRI, as noted above. For a given TR (500 ms), UTE images were acquired at a series of TEs of 0.1, 0.25, 0.5, 1, 2.5, 5, 10, and 15 ms.

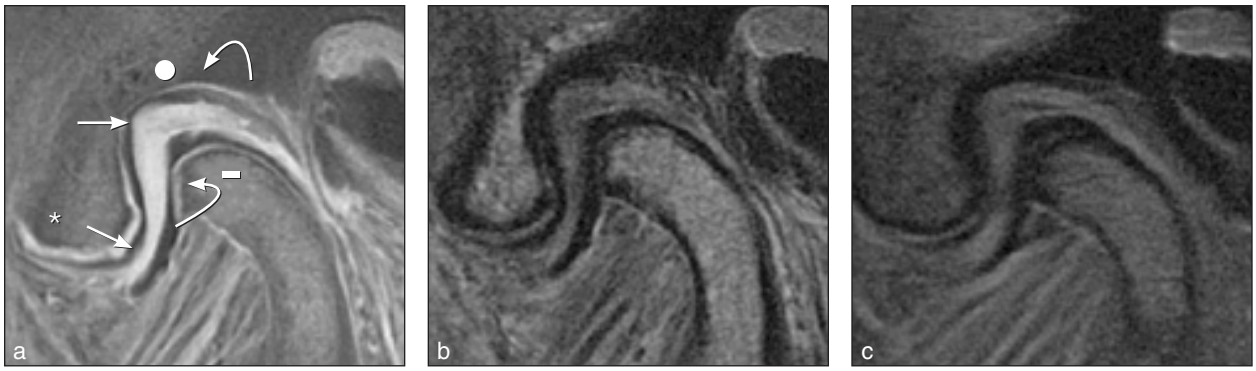

Fig 1 *(a)* UTE (TR = 500 ms, TE = 8 μs / 6.6 ms), *(b)* T1-weighted (TR = 500 ms, TE = 15 ms), and *(c)* proton density-weighted fat-suppressed (TR = 1,800 ms, TE = 11.7 ms) MR images of the TMJ in a cadaveric specimen show increased signal in the TMJ disc *(straight arrows)* situated between the articular eminence *(asterisk)*, mandibular fossa *(circle)*, and mandibular condyle *(rectangle)* on the UTE MR image. The fibrocartilaginous articular surfaces *(curved arrows)* of the condyle and mandibular fossa are also characterized by linear bright signal intensity. The UTE MR sequence facilitates identification of these short T2 tissues through acquiring signal from them, not afforded by the standard clinical sequences.

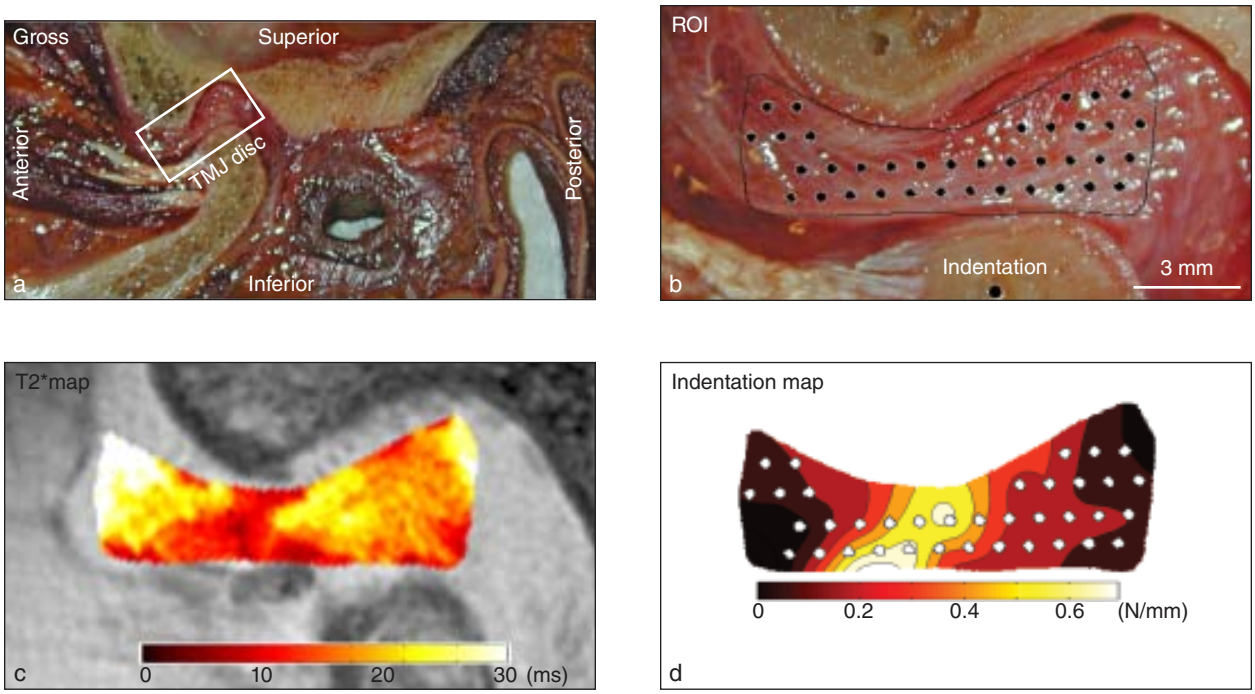

Fig 2 TMJ specimen slice was subjected to (a) quantitative MRI and (b) biomechanical indentation testing, and analyzed to yield (c) a T2* map and (d) indentation stiffness map of the sample TMJ disc. A general inverse relation between T2* and stiffness values are apparent.

Matlab (R2009a with Image Processing Toolbox) was used to take MR images at multiple TEs that were analyzed by voxel-wise mono-exponential fitting of signal intensity to: $S(TE) = S_0 \cdot \exp(-TE/T2^*)$. This, along with masks representing areas of the TMJ disc (created using Adobe Photoshop), provided T2* maps. The total scan duration for all of the ex vivo sequences was ~50 min.

Two ex vivo reference standards were explored in this study. One tissue slice was compared to indentation testing (Figs 2 and 3) and the second slice was compared to histologic evaluation (Fig 4).

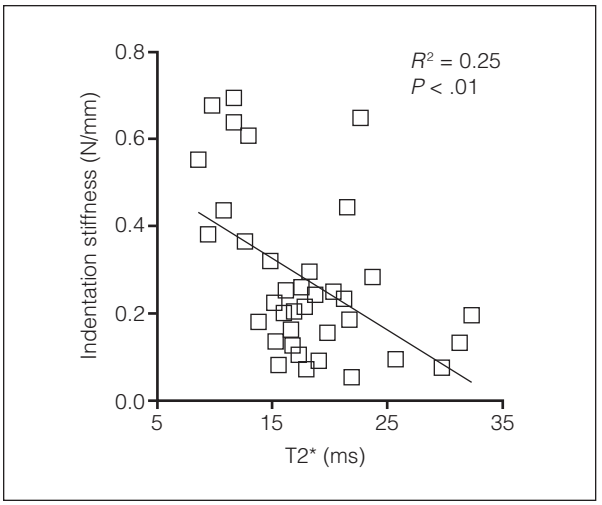

Fig 3 Indentation stiffness of the TMJ disc was correlated with regional T2* values. A significant inverse relationship was found, where a high T2* value was associated with softer disc, suggesting possible deterioration.

In Vivo MRI Evaluation

The left TMJs of two asymptomatic volunteers (both 37-year-old males) were imaged (Fig 5) using a three-dimensional (3D) UTE MRI sequence and employing a short hard pulse (40 μs) followed by 3D radial sampling. A 3-inch surface coil was placed adjacent to the volunteer's TMJ. The following scanning parameters were used: TR = 21 ms; TE = 0.008, 4, 8, and 12 ms; matrix = 384 × 384 × 384; FOV = $(14\ cm)^3$; voxel size = $(0.36\ mm)^3$; readout = 256; number of projections = 30,000; bandwidth = ± 62.5 kHz; flip angle = 8 degrees; and scan time = 13 minutes. SNR was determined by comparing the signal intensity in the TMJ disc to that in the background. T2* was quantified in the sagittal plane to create maps and to determine the average values for the whole TMJ disc. For each volunteer, three image slices (central where mandibular condyle appears the largest, 3.6 mm to the left, and 3.6 mm to the right) were analyzed.

Biomechanical Testing

Indentation testing, a nondestructive biomechanical test,[22,23] was used on the TMJ disc. A sample slice (Fig 2a) was placed on a flat stage and secured at the articular fossa and the mandibular condyle, and the TMJ disc at multiple sites was subjected to indentation testing (Fig 2b) using a benchtop apparatus (V500cs, Biomomentum) fitted with a 0.8-mm-diameter plane-ended tip. The stage was equipped with an x–y translation indexer (0.01-mm resolution) to allow for a high-precision positioning of indentation sites. Throughout testing, the sample was kept hydrated using phosphate buffered saline containing proteinase inhibitors.[24] The indentation protocol consisted of application of a small tare load (~0.15 g) followed by ramp compression of 100 μm (at 100 μm/s). The load was held for 1 s, and unloaded at the same rate. Indentation stiffness (higher value indicates stiffer sample) was determined from load-displacement data and converted to the units of N/mm, as has been previously described.[25] Additionally, a map of indentation stiffness was created in Matlab by using contour-plot of stiffness values at each indentation site, and applying the mask created for T2* mapping.

MR-Biomechanics Correlation

The T2* (Fig 2c) and indentation stiffness maps (Fig 2d) were co-registered, and at each indentation site, ROIs approximately the size of the indenter tip were created to determine average T2* value at the site. Pearson correlation was used to associate indentation stiffness to T2* values, with significance level set at $\alpha = 0.05$.

Histology

For histopathology, the discal tissue was processed to evaluate tissue morphology and composition. Tissue was fixed in buffered 10% formalin and paraffin embedded. Five micrometer sections were cut with a microtome and were stained with safranin-O and fast green for glycosaminoglycan (GAG) distribution and with Picrosirius red for polarized light microscopy (PLM) for a better evaluation of the tissue morphology. Birefringence and fiber orientation were assessed using quantitative PLM[26,27]; a slide with an unstained tissue section (to reduce background noise) was centered on a rotating stage of an Olympus BX60 microscope and rotated from

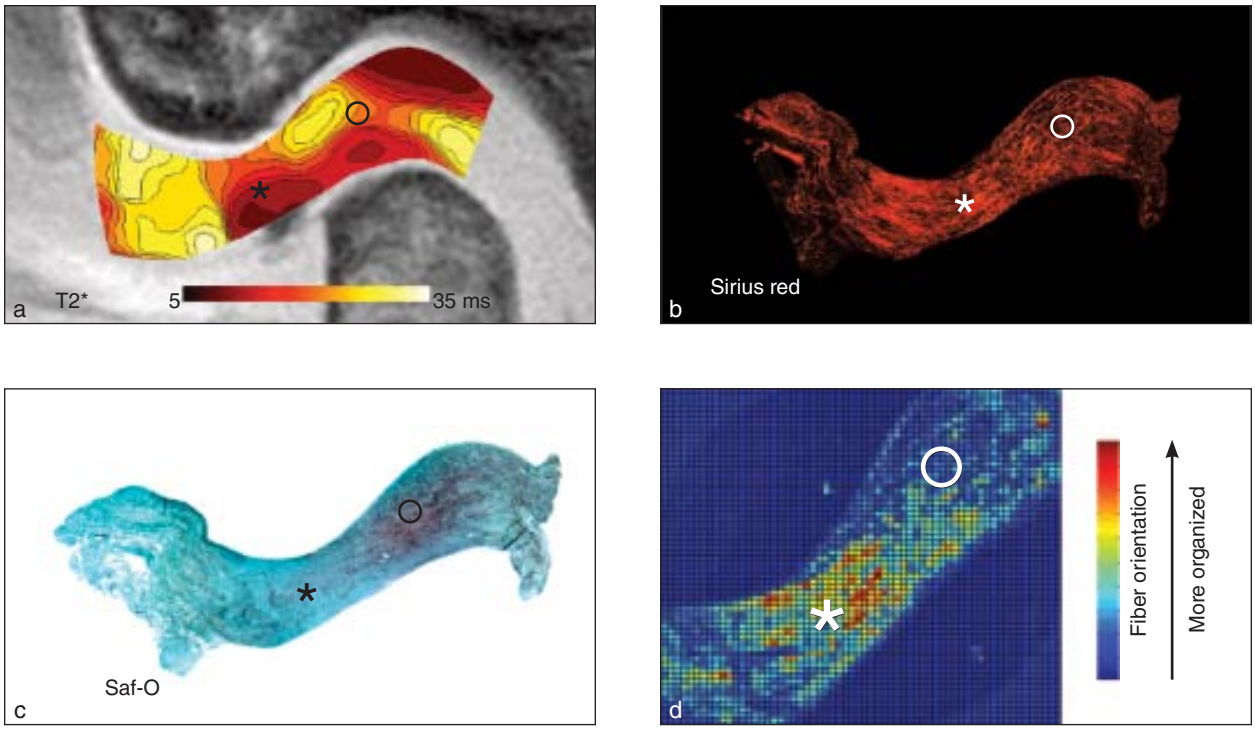

Fig 4 Correspondence between MRI and histologic measures in a TMJ disc. *(a)* T2* map of the TMJ disc was compared with its *(b)* sirius red staining, *(c)* safranin-O (Saf-O) and fast green staining, and *(d)* a heat map for fiber orientation obtained by using qPLM methods. * represents the central region with low T2* value, less safranin-O staining, and greater collagen orientation. O represents posterior region with the opposite characteristics.

0 to 100 degrees while 21 images were captured in 5 degree increments. A custom Matlab program was created to determine the birefringence and fiber orientation. A higher birefringence signal indicates higher fiber organization. Birefringence and fiber orientation are presented in heat maps where a brighter signal (red-yellow) correlates with higher birefringence and fiber organization and the lower signal (light blue) correlates with more disorganized fibers. Fiber orientation can be determined from a heat map where each color corresponds to degrees of rotation. For example, dark blue = 0 degrees, yellow = 45 degrees, and dark red = 90 degrees. The micrographs and PLM maps were compared to the UTE T2* map to compare spatial patterns of the measures.

Results

On visual inspection, the disc tissue appeared low in signal intensity (black appearance referred to as signal void) on the T1- and proton density-weighted sequences (Figs 1b and 1c). On the UTE MR image (Fig 1a), discal tissue demonstrated increased signal (bright appearance), which allowed for its distinction from surrounding tissues as well as for its morphologic characterization. Mean SNR values of the TMJ disc supported this observation and were 14.2, 18.2, and 41.6 on the T1-weighted sequence, proton density-weighted fat-suppressed sequence, and UTE MR sequence, respectively.

Use of the Constant TR–Varying TE technique in conjunction with UTE imaging produced a T2* map of the TMJ disc (Figs 2c and 4c). The average T2* value of the two discs was 17.3 ± 1.7 ms.

In the evaluation of the stiffness of the disc by biomechanical testing, a general inverse relationship between the T2* values and the indentation stiffness of the tissue was noted qualitatively in the maps (Figs 2c and 2d). Higher T2* values were associated with softer regions of the disc (Fig 3, $P < .001$, $R^2 = 0.25$) with possible tissue degeneration or deterioration.

When the T2* map was compared with histologic measures, the central region with lower T2* values (Fig 4a) corresponded with less GAG staining (Fig 4c) and greater collagen fiber organization seen with Picrosirius red stain (Fig 4b) and the heat map for fiber orientation (Fig 4d). In contrast, the posterior region with higher T2* values exhibited the opposite trend.

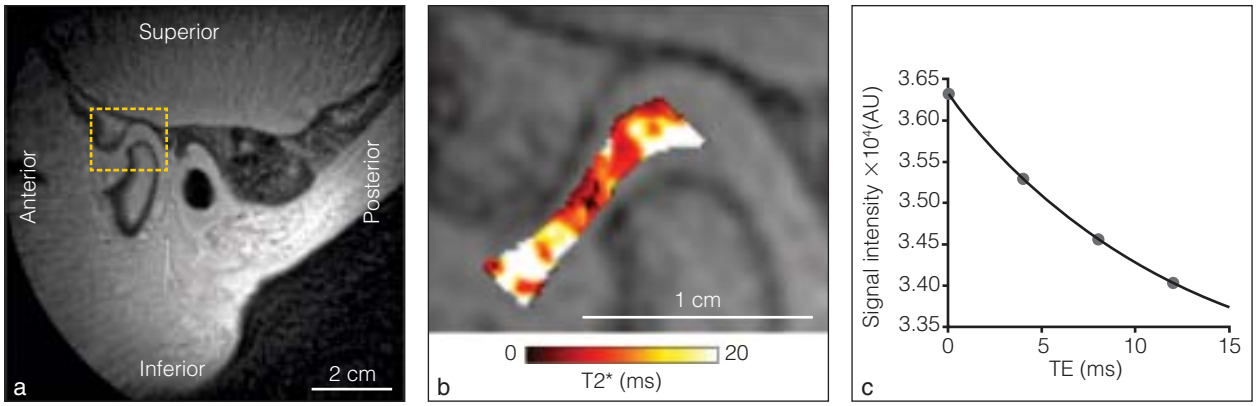

Fig 5 *(a)* Left TMJ of a volunteer was imaged quantitatively using a 3D UTE MRI sequence, and analyzed to yield a *(b)* T2* map. *(c)* Graph showing goodness of the fit during the fitting.

The in vivo 3D UTE MR images (Fig 5a) of the TMJ from the volunteers also exhibited low noise (average SNR = 20.8) and revealed high intensity in the region of the TMJ disc. Maps revealed spatial variations in the T2* values (Fig 5b), with an average T2* value of 11.8 ± 6.3 ms, which was similar to those in the ex vivo specimens (ANOVA $P = .3$). The quality of the fitting, averaged over the ROI, was good in all cases (Fig 5c).

Discussion

TMJ pathology affects a significant portion of the population at some stage in their lives.[7,28,29] These disorders that present as painful functional disturbance have a complex etiology, most recently encompassed by biopsychosocial models.[3,4] In part, these disorders have been attributed to muscular dysfunction at and around the joint and internal derangement of the joint.[2] In the latter, intra-articular components, most notably the disc and cartilage, can be affected.[8] Progression of TMJ internal derangement may even lead to perforation of the disc and, ultimately, to osseous remodeling that is more obvious in the condyle than in mandibular fossa and articular eminence.[30,31] For this reason, noninvasive assessment of the TMJ could be important in characterizing tissue and monitoring tissue changes through the progression of acute to chronic disease, as well as monitoring tissue response to therapy.[9]

The TMJ differs from other synovial joints in that fibrocartilage covers the articular surfaces instead of hyaline cartilage. The fibrocartilaginous disc is the most important functional part of the joint and has similarities with the meniscus of the knee in its composition of collagen I and II, glycosaminoglycans, and water.[32] Unlike the meniscus of the knee, the TMJ disc has a significant component of elastic fibers that may vary with age.[33,34]

MRI has gained wide acceptance in current imaging evaluation of the TMJ due to its excellent soft tissue contrast and multiplanar imaging capabilities. The basic MRI evaluation of the TMJ has mainly focused on the disc, its morphology, and position relative to the condyle and articular eminence with an open- and closed-mouth position, and on its intrinsic signal intensity. Debate exists with several reports over the signal intensity of the TMJ disc. It has been reported that the normal TMJ disc has a low signal intensity throughout and, as the TMJ disc degenerates, it becomes high in signal intensity.[35,36] Other reports have described the normal TMJ with intermediate to high signal intensity on T1-weighted MR images, with decreasing signal intensity with degeneration.[37] Most recently, increased signal intensity on proton density-weighted fat-suppressed and T1-weighted sequences within the posterior band of the TMJ disc has been described in the setting of tissue degeneration.[38] Although standard clinical MR sequences at 1.5 T appear to be effective in accurate characterization of disc morphology and position,[39–45] there is a definite need for studies on the diagnostic efficacy of MRI in TMJ disease.[46]

Novel MRI techniques have been attempted to better evaluate the TMJ. Stehling et al have used 3.0 T in their studies and concluded that with higher SNR as compared with 1.5 T, depiction of TMJ anatomy benefits significantly.[8] However, a limitation in their study was the lack of a gold standard and direct comparison with 1.5 T imaging. Hayakawa et al processed routine TMJ MRI slices by tissue segmentation followed by 3D reconstruction with visualization software in a 1.5 T MR unit.

This technique focused on displacement and morphology of the disc rather than its signal intensity.[10] Similarly, Wang et al evaluated discal displacement in their studies with dynamic half-Fourier acquired single-shot turbo spin-echo (HASTE) using parallel imaging and comparison with static proton density imaging.[11] Initial exploration of diffusion-weighted MR imaging has been introduced for the ultimate characterization of the stages of inflammation, but the details of the disc were unidentifiable.[47]

Alhough MRI provided the initial steps toward noninvasive evaluation of the structural components of the TMJ, its intrinsic tissue characteristics necessitated more specific advances. The fibrocartilaginous nature of the articular surfaces and disc suggest that these tissues have a relatively short intrinsic T2 (MRI characteristic intrinsic and specific to all tissues), making them incompletely detected by standard clinical sequences and unable to be accurately quantified with standard T2 measurement techniques.

UTE pulse sequences allow a signal from short T2 tissues to be detected and have the ability to provide quantitative assessment for tissues with predominantly short T2 tissue components in the clinical setting for the first time. The gradient echo techniques such as 2D or 3D fast spoiled gradient recalled echo have the ability to measure T2 values in the 1- to 2-ms range, although they do so at the expense of resolution, requiring large FOV and increased slice thickness and bandwidth. This compromise is unacceptable for tissues such as the TMJ disc, as they require high resolution to localize tissue for the purposes of sampling. The UTE sequences were originally implemented by Bergin et al in 1991.[48] Since their first introduction, the minimum TE has progressively decreased from 150 μs to 80 μs and recently to 8 μs, although the precise definition of TE for short T2 tissue components is still a matter of debate.[48–50] The present study has served to provide a means to apply the UTE MRI sequence to the tissues of the TMJ, thereby allowing a signal to be obtained from the TMJ disc. This has facilitated excellent visual characterization of the TMJ disc compared to the standard clinical sequences in vitro. Further, it has allowed for T2* quantification of the TMJ disc. It appears that T2* values when compared with histologic evaluation do provide a noninvasive means to reflect structural alteration within the tissue. The lower T2* values in this study's specimen reflected fibrous change. In addition, while the described UTE method is based on gradient echo imaging, the authors are currently developing a spin-echo–based UTE method that could be used to determine T2 values, rather than T2*. This will further expand the utility of quantitative UTE methods.

Biomechanical properties of TMJ articular tissues have been of interest, for establishment of baseline values[51–53] as well as for tissue engineering.[32] Little knowledge is available of the biomechanical properties of human samples, nor changes that may occur with pathology of TMJ tissues. Biomechanical property changes are likely to occur during TMJ degeneration, which can result in degenerative changes histologically.[54] Similarly, degeneration in human articular cartilage results in altered biomechanical properties.[22,55,56] It should be noted that the indentation in this study was not applied in the physiologic direction (ie, superior to inferior direction on the intact surface of the disc). This may have resulted in a lowered stiffness than compressing an intact disc in a physiologic direction, since superficial collagen fibrils of an intact tissue provide resistance to compression, analogous to the workings of a trampoline. Nonetheless, the indentation test used in this study still captured topographic variations in disc stiffness, which are useful for determining local changes in the tissue.

Indentation testing is a nondestructive and sensitive testing method for TMJ articular tissues. Indentation is performed by compressing the sample surface a small amount with a tip (~ < 1 mm diameter) while load is measured. Indentation has been used for TMJ testing, although not as widely as tensile testing,[52,53,57] which is destructive. Since the normal TMJ disc has topographical variations in mechanical properties,[52,57] assessment in multiple regions is important for correct interpretation of the biomechanical evaluation. In that regard, indentation testing is advantageous since it can be performed rapidly (~seconds) and facilitates multiple-site testing. More importantly, if additional analysis (eg, histology) is desired, a nondestructive method is required. Indentation testing is sensitive to minute changes in structure[22] and composition (ie, glycosaminoglycan content[58]) of cartilage near the contact surface, and is likely to be sensitive to biomechanical changes in fibrocartilaginous tissues of the TMJ as well. The relationship between the function of the TMJ articular fibrocartilage and disc as determined by biomechanical testing and the structural components of these tissues has not been determined. There is increasing interest in the possibility of relating noninvasive quantitative MR evaluation of tissue to its functional competence; the present preliminary study found a weak but statistically significant correlation between MR and indentation properties, and additional samples will reveal if this relationship holds true.

The present study with UTE MRI at 3T allowed visualization of the TMJ disc of the mandibular condyle with high spatial resolution and signal, thereby

allowing for its easy identification and quantitative T2* characterization in vitro. The study also established the feasibility of quantitative UTE T2* evaluation in vivo, although additional work is required to optimize the image contrast needed for morphologic evaluation. Further, the present results suggest that UTE quantitative MRI may reflect structural properties as determined by histology, as well as functional changes as reflected by indentation testing. While the authors realize the study is limited by the small specimen number, the data provide a promising platform for future study.

Acknowledgments

This study was supported in parts by Veterans Affairs (VA) Research and National Institutes of Health (NIH) R21 DE019008 (CBC) as well as NIH K01 AR059764 (WCB). Authors would like to thank Professor Darryl D. D'Lima and Nick Steklov for quantitative PLM analysis.

References

1. Alomar X, Medrano J, Cabratosa J, et al. Anatomy of the temporomandibular joint. Semin Ultrasound CT MR 2007;28: 170–183.
2. Hayt MW, Abrahams JJ, Blair J. Magnetic resonance imaging of the temporomandibular joint. Top Magn Reson Imaging 2000;11:138–146.
3. Klasser GD, Greene CS. The changing field of temporomandibular disorders: What dentists need to know. J Can Dent Assoc 2009;75:49–53.
4. Ahmad M, Hollender L, Anderson Q, et al. Research diagnostic criteria for temporomandibular disorders (RDC/TMD): Development of image analysis criteria and examiner reliability for image analysis. Oral Surg Oral Med Oral Pathol Oral Radiol Endod 2009;107:844–860.
5. Ren YF, Westesson PL, Isberg A. Magnetic resonance imaging of the temporomandibular joint: Value of pseudodynamic images. Oral Surg Oral Med Oral Pathol Oral Radiol Endod 1996;81:110–123.
6. Cavalcanti MG, Lew D, Ishimaru T, Ruprecht A. MR imaging of the temporomandibular joint: A validation experiment in vitro. Acad Radiol 1999;6:675–679.
7. Chirani RA, Jacq JJ, Meriot P, Roux C. Temporomandibular joint: A methodology of magnetic resonance imaging 3-D reconstruction. Oral Surg Oral Med Oral Pathol Oral Radiol Endod 2004;97:756–761.
8. Stehling C, Vieth V, Bachmann R, et al. High-resolution magnetic resonance imaging of the temporomandibular joint: Image quality at 1.5 and 3.0 tesla in volunteers. Invest Radiol 2007;42:428–434.
9. Vilanova JC, Barcelo J, Puig J, Remollo S, Nicolau C, Bru C. Diagnostic imaging: Magnetic resonance imaging, computed tomography, and ultrasound. Semin Ultrasound CT MR 2007;28:184–191.
10. Hayakawa Y, Kober C, Otonari-Yamamoto M, Otonari T, Wakoh M, Sano T. An approach for three-dimensional visualization using high-resolution MRI of the temporomandibular joint. Dentomaxillofac Radiol 2007;36:341–347.
11. Wang EY, Mulholland TP, Pramanik BK, et al. Dynamic sagittal half-Fourier acquired single-shot turbo spin-echo MR imaging of the temporomandibular joint: Initial experience and comparison with sagittal oblique proton-attenuation images. AJNR Am J Neuroradiol 2007;28:1126–1132.
12. Shimazaki Y, Saito K, Matsukawa S, et al. Image quality using dynamic MR imaging of the temporomandibular joint with true-FISP sequence. Magn Reson Med Sci 2007;6: 15–20.
13. Abolmaali ND, Schmitt J, Schwarz W, Toll DE, Hinterwimmer S, Vogl TJ. Visualization of the articular disk of the temporomandibular joint in near-real-time MRI: Feasibility study. Eur Radiol 2004;14:1889–1894.
14. Tomura N, Otani T, Narita K, et al. Visualization of anterior disc displacement in temporomandibular disorders on contrast-enhanced magnetic resonance imaging: Comparison with T2-weighted, proton density-weighted, and precontrast T1-weighted imaging. Oral Surg Oral Med Oral Pathol Oral Radiol Endod 2007;103:260–266.
15. Hall-Craggs MA, Porter J, Gatehouse PD, Bydder GM. Ultrashort echo time (UTE) MRI of the spine in thalassaemia. Br J Radiol 2004;77:104–110.
16. Reichert IL, Benjamin M, Gatehouse PD, et al. Magnetic resonance imaging of periosteum with ultrashort TE pulse sequences. J Magn Reson Imaging 2004;19:99–107.
17. Reichert IL, Robson MD, Gatehouse PD, et al. Magnetic resonance imaging of cortical bone with ultrashort TE pulse sequences. Magn Reson Imaging 2005;23:611–618.
18. Robson MD, Gatehouse PD, Bydder M, Bydder GM. Magnetic resonance: An introduction to ultrashort TE (UTE) imaging. J Comput Assist Tomogr 2003;27:825–846.
19. Robson MD, Bydder GM. Clinical ultrashort echo time imaging of bone and other connective tissues. NMR Biomed 2006; 19:765–780.
20. Gatehouse PD, Bydder GM. Magnetic resonance imaging of short T2 components in tissue. Clin Radiol 2003;58:1–19.
21. Tyler DJ, Robson MD, Henkelman RM, Young IR, Bydder GM. Magnetic resonance imaging with ultrashort TE (UTE) PULSE sequences: Technical considerations. J Magn Reson Imaging 2007;25:279–289.
22. Bae WC, Temple MM, Amiel D, Coutts RD, Niederauer GG, Sah RL. Indentation testing of human cartilage: Sensitivity to articular surface degeneration. Arthritis Rheum 2003; 48:3382–3394.
23. Lyyra T, Kiviranta I, Vaatainen U, Helminen HJ, Jurvelin JS. In vivo characterization of indentation stiffness of articular cartilage in the normal human knee. J Biomed Mater Res 1999; 48:482–487.
24. Frank EH, Grodzinsky AJ. Cartilage electromechanics-II. A continuum model of cartilage electrokinetics and correlation with experiments. J Biomech 1987;20:629–639.
25. Bae WC, Law AW, Amiel D, Sah RL. Sensitivity of indentation testing to step-off edges and interface integrity in cartilage repair. Ann Biomed Eng 2004;32:360–369.
26. Nieminen MT, Rieppo J, Toyras J, et al. T2 relaxation reveals spatial collagen architecture in articular cartilage: A comparative quantitative MRI and polarized light microscopic study. Magn Reson Med 2001;46:487–493.
27. Rieppo J, Hallikainen J, Jurvelin JS, Helminen HJ, Hyttinen MM. Novel quantitative polarization microscopic assessment of cartilage and bone collagen birefringence, orientation and anisotropy [abstract]. Trans Orthop Res Soc 2003;28:570.

28. Greene AR. TMJ and the test of time. Quintessence Int Dent Dig 1982;13:1255–1257.
29. Whyte AM, McNamara D, Rosenberg I, Whyte AW. Magnetic resonance imaging in the evaluation of temporomandibular joint disc displacement. A review of 144 cases. Int J Oral Maxillofac Surg 2006;35:696–703.
30. Emshoff R, Rudisch A. Are internal derangement and osteoarthrosis linked to changes in clinical outcome measures of arthrocentesis of the temporomandibular joint? J Oral Maxillofac Surg 2003;61:1162–1170.
31. Lieberman JM, Gardner CL, Motta AO, Schwartz RD. Prevalence of bone marrow signal abnormalities observed in the temporomandibular joint using magnetic resonance imaging. J Oral Maxillofac Surg 1996;54:434–440.
32. Detamore MS, Orfanos JG, Almarza AJ, French MM, Wong ME, Athanasiou KA. Quantitative analysis and comparative regional investigation of the extracellular matrix of the porcine temporomandibular joint disc. Matrix Biol 2005;24:45–57.
33. Clement C, Bravetti P, Plenat F, et al. Quantitative analysis of the elastic fibres in the human temporomandibular articular disc and its attachments. Int J Oral Maxillofac Surg 2006; 35:1120–1126.
34. Leonardi R, Villari L, Bernasconi G, Caltabiano M. Histochemical study of the elastic fibers in pathologic human temporomandibular joint discs. J Oral Maxillofac Surg 2001;59: 1186–1192.
35. Katzberg RW, Tallents RH. Normal and abnormal temporomandibular joint disc and posterior attachment as depicted by magnetic resonance imaging in symptomatic and asymptomatic subjects. J Oral Maxillofac Surg 2005;63:1155–1161.
36. Schellhas KP, Fritts HM, Heithoff KB, Jahn JA, Wilkes CH, Omlie MR. Temporomandibular joint: MR fast scanning. Cranio 1988;6:209–216.
37. Helms CA, Kaban LB, McNeill C, Dodson T. Temporomandibular joint: Morphology and signal intensity characteristics of the disk at MR imaging. Radiology 1989;172:817–820.
38. Orhan K, Arslan A, Kocyigit D. Temporomandibular joint osteochondritis dissecans: Case report. Oral Surg Oral Med Oral Pathol Oral Radiol Endod 2006;102:e41–46.
39. Benbelaid R, Fleiter B, Zouaoui A, Gaudy JF. Proposed graphical system of evaluating disc-condyle displacements of the temporomandibular joint in MRI. Surg Radiol Anat 2005;27:361–367.
40. Emshoff R, Rudisch A, Innerhofer K, Brandlmaier I, Moschen I, Bertram S. Magnetic resonance imaging findings of internal derangement in temporomandibular joints without a clinical diagnosis of temporomandibular disorder. J Oral Rehabil 2002;29:516–522.
41. Foucart JM, Pajoni D, Carpentier P, Pharaboz C. MRI study of temporomandibular joint disk behavior in chilren with hyperpropulsion appliances. Orthod Fr 1998;69:79–91.
42. Milano V, Desiate A, Bellino R, Garofalo T. Magnetic resonance imaging of temporomandibular disorders: Classification, prevalence and interpretation of disc displacement and deformation. Dentomaxillofac Radiol 2000;29:352–361.
43. Rao VM, Bacelar MT. MR imaging of the temporomandibular joint. Neuroimaging Clin N Am 2004;14:761–775.
44. Schmitter M, Kress B, Ludwig C, Koob A, Gabbert O, Rammelsberg P. Temporomandibular joint disk position assessed at coronal MR imaging in asymptomatic volunteers. Radiology 2005;236:559–564.
45. Yamada I, Murata Y, Shibuya H, Suzuki S. Internal derangements of the temporomandibular joint: Comparison of assessment with three-dimensional gradient-echo and spin-echo MRI. Neuroradiology 1997;39:661–667.
46. Limchaichana N, Petersson A, Rohlin M. The efficacy of magnetic resonance imaging in the diagnosis of degenerative and inflammatory temporomandibular joint disorders: A systematic literature review. Oral Surg Oral Med Oral Pathol Oral Radiol Endod 2006;102:521–536.
47. Otonari T, Wakoh M, Sano T, Yamamoto M, Ohkubo M, Harada T. Parameters for diffusion weighted magnetic resonance imaging for temporomandibular joint. Bull Tokyo Dent Coll 2006;47:5–12.
48. Bergin CJ, Pauly JM, Macovski A. Lung parenchyma: Projection reconstruction MR imaging. Radiology 1991;179: 777–781.
49. Bredella MA, Tirman PF, Peterfy CG, et al. Accuracy of T2-weighted fast spin-echo MR imaging with fat saturation in detecting cartilage defects in the knee: Comparison with arthroscopy in 130 patients. AJR Am J Roentgenol 1999;172: 1073–1080.
50. Gold GE, Thedens DR, Pauly JM, et al. MR imaging of articular cartilage of the knee: New methods using ultrashort TEs. AJR Am J Roentgenol 1998;170:1223–1226.
51. Tanne K, Tanaka E, Sakuda M. The elastic modulus of the temporomandibular joint disc from adult dogs. J Dent Res 1991; 70:1545–1548.
52. Kim KW, Wong ME, Helfrick JF, Thomas JB, Athanasiou KA. Biomechanical tissue characterization of the superior joint space of the porcine temporomandibular joint. Ann Biomed Eng 2003;31:924–930.
53. Tanaka E, Tanaka M, Hattori Y, et al. Biomechanical behaviour of bovine temporomandibular articular discs with age. Arch Oral Biol 2001;46:997–1003.
54. Luder HU. Factors affecting degeneration in human temporomandibular joints as assessed histologically. Eur J Oral Sci 2002;110:106–113.
55. Akizuki S, Mow VC, Muller F, Pita JC, Howell DS, Manicourt DH. Tensile properties of human knee joint cartilage: I. Influence of ionic conditions, weight bearing, and fibrillation on the tensile modulus. J Orthop Res 1986;4:379–392.
56. Roberts S, Weightman B, Urban J, Chappell D. Mechanical and biochemical properties of human articular cartilage in osteoarthritic femoral heads and in autopsy specimens. J Bone Joint Surg Br 1986;68:278–288.
57. Detamore MS, Athanasiou KA. Tensile properties of the porcine temporomandibular joint disc. J Biomech Eng 2003; 125:558–565.
58. Samosky JT, Burstein D, Eric Grimson W, Howe R, Martin S, Gray ML. Spatially-localized correlation of dGEMRIC-measured GAG distribution and mechanical stiffness in the human tibial plateau. J Orthop Res 2005;23:93–101.